TEMPERATURE-DEPENDENT DISPLACEMENT EFFICIENCY IN RESONANCE-CONTROLLED ULTRASONIC VHCF TESTING OF DUPLEX STAINLESS STEEL EN 1.4462

Lukas GARALIS, Nikolaj VIŠNIAKOV

Vilnius Gediminas Technical University, Vilnius, Lithuania, EU, lukas.garalis@vilniustech.lt

https://doi.org/10.37904/metal.2026.5245

Abstract

The influence of specimen temperature on displacement efficiency was investigated for duplex stainless steel EN 1.4462 using a 20 kHz ultrasonic fatigue testing system. Resonance-controlled tests were conducted over incremental excitation levels defined by the function generator output voltage (VPP), with continuous phase control to maintain stable resonance. Axial displacement amplitude, resonant frequency, phase difference, and specimen temperature were continuously recorded. Displacement efficiency was defined as the ratio of displacement amplitude to excitation level (µm/VPP). During testing, specimen temperature increased from approximately 29 °C to 90–100 °C, depending on excitation level and cooling conditions. Peak temperatures exceeding 100 °C were observed in high-load tests above 1.5 VPP, corresponding to displacement amplitudes above 13 µm. Over this range, a consistent downward shift in resonant frequency of approximately 200–250 Hz (1–1.3%) was measured, indicating temperature-induced reductions in effective dynamic stiffness. Displacement efficiency showed a strong temperature dependence. Under well-cooled conditions, increases in excitation produced substantial displacement gains, while excessive cooling caused resonance instability, whereas at elevated temperatures progressively higher excitation was required to achieve equivalent displacement, indicating diminishing returns due to reduced elastic stiffness and increased dissipation. At fixed excitation levels, displacement amplitudes varied by up to 10% depending on phase, with stable resonance and maximum displacement confined to a narrow phase window of 0–2°. These findings demonstrate that temperature- and phase-dependent effects govern ultrasonic displacement response, underscoring the need for temperature- and phase-aware displacement calibration in ultrasonic VHCF testing of duplex stainless steels.

Keywords: Ultrasonic very high cycle fatigue, resonance behaviour, thermo-mechanical coupling, temperature effects, 1.4462 steel

1. INTRODUCTION

Ultrasonic fatigue testing at ~20 kHz enables very high cycle fatigue (VHCF) investigations up to 10^9 cycles within practical timeframes and is widely used for studying gigacycle fatigue behaviour [1,2]. The method relies on operation at mechanical resonance, making the system response highly sensitive to variations in material properties and test conditions [2,3]. During ultrasonic loading, internal damping leads to self-heating of the specimen, which modifies its effective stiffness and damping characteristics [1,2]. As a result, resonance frequency shifts and displacement amplitude changes even under constant excitation [2,3]. This coupling between thermal and mechanical response becomes increasingly significant at higher excitation levels, where temperature rise is substantial and directly affects system stability and response [1,2,4,5]. Despite this well-recognized thermo-mechanical coupling, temperature effects are often not explicitly accounted for in displacement-based calibration procedures used in ultrasonic fatigue testing [5,6]. This can introduce uncertainty in stress estimation and reduce reproducibility, particularly under varying cooling conditions. The present study investigates the influence of temperature on displacement efficiency in a resonance-controlled ultrasonic fatigue system. The relationships between excitation level, displacement amplitude, resonance frequency, and phase stability are analysed for duplex stainless steel EN 1.4462, with the aim of improving calibration reliability under thermally evolving conditions.

2. MATERIALS AND METHODS

The investigated material was cold-drawn duplex stainless steel EN 1.4462. Specimens were manufactured in an hourglass geometry to ensure maximum stress localization within the gauge section under resonance conditions as shown in **Figure 1**. The geometry was specifically designed to match the first longitudinal resonance mode at approximately 20 kHz. The surface condition was carefully controlled through final fine machining.

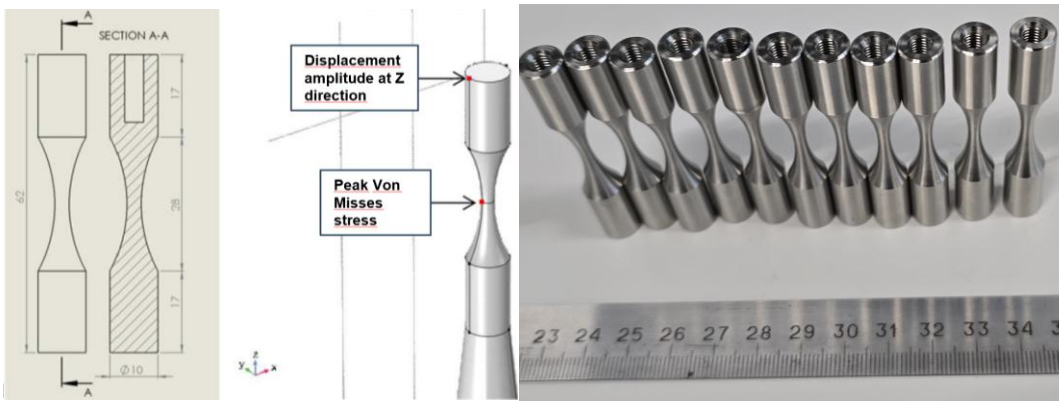

Figure 1 Specimen geometry and stress–displacement locations

Fatigue experiments were performed using a resonance-based ultrasonic testing system operating at a nominal frequency of around 20 kHz. A schematic representation of the experimental setup is shown in **Figure 2**, including the actuation chain, measurement system, and control architecture.

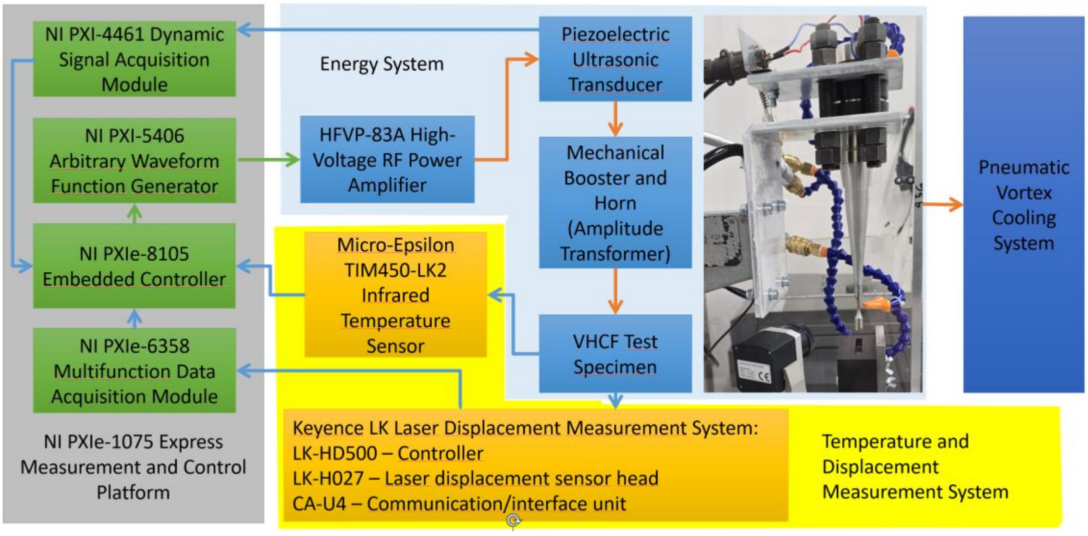

Figure 2 Resonance-based ultrasonic testing system architecture

The system comprised a piezoelectric ultrasonic transducer, an aluminum booster, and an aluminum horn forming a longitudinal vibration chain that transmits displacement to the specimen. Excitation was provided by a function generator and amplified using a high-voltage RF power amplifier (HFVP-83A). Control and data acquisition were performed via a National Instruments PXI system, enabling synchronized excitation, measurement, and real-time feedback.

Axial displacement at the specimen tip was measured using a laser displacement sensor (Keyence LK-H027 with LK-HD500 controller), while specimen temperature was monitored by an infrared sensor (Micro-Epsilon TIM450-LK2). The system continuously recorded displacement amplitude, excitation voltage, frequency, phase difference, and temperature. Resonance of the coupled system was governed by nonlinear stiffness effects and maintained using phase-based control, where the phase difference between excitation (voltage) and response (current) was tracked. Testing was conducted under displacement-controlled conditions using incremental excitation levels (VPP). An initial frequency sweep (19–21 kHz) identified the resonance region, followed by phase-controlled backward sweeps to stabilize resonance within a narrow phase range (~0°–20°). Backward sweeping ensured stable convergence under nonlinear response conditions. At each excitation level, data were recorded after reaching quasi-steady thermal and resonance conditions. Displacement efficiency (µm/VPP) was used to characterize the electromechanical response. Cooling was applied using a pneumatic vortex system with adjustable airflow. Stable operation was maintained via continuous phase tracking and frequency adjustment (0°–3° phase range). All measurements were performed on a single specimen to eliminate inter-specimen variability.

3. RESULTS AND DISCUSSION

The relationship between excitation level and specimen temperature is shown in Figure 3. A strong nonlinear increase in temperature with increasing function generator output voltage (VPP) is observed across all cooling conditions. At low excitation levels (<1 VPP), the specimen temperature remains close to ambient (~30 °C), indicating negligible self-heating. However, beyond approximately 1.5 VPP, temperature rises rapidly, exceeding 90–100 °C at high excitation levels. Cooling pressure influences the rate of temperature increase but does not fundamentally alter the overall trend. Higher cooling pressures delay temperature rise slightly, but at elevated excitation levels, thermal accumulation dominates. This confirms that internal damping and cyclic deformation are the dominant sources of heat generation in the ultrasonic system.

The effect of temperature on resonance frequency is presented in **Figure 4**. A clear monotonic decrease in resonance frequency with increasing temperature is observed, with a total shift of approximately 200–250 Hz over the investigated range (30–105 °C).

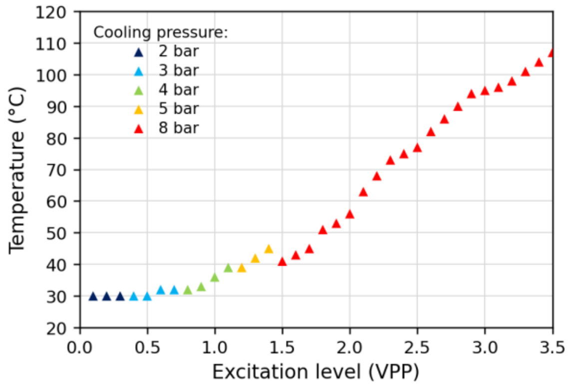

Figure 3 Specimen temperature as a function of excitation level under different cooling pressures

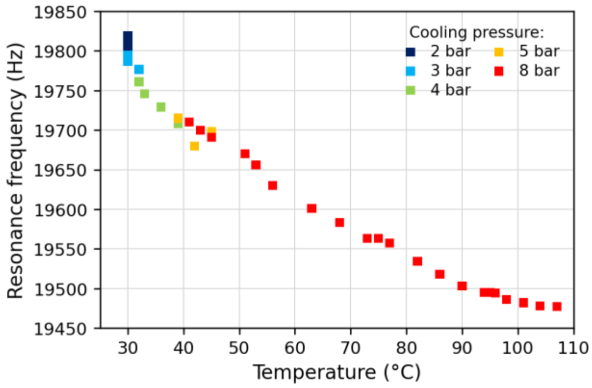

Figure 4 Resonance frequency as a function of specimen temperature under different cooling pressures

This corresponds to a relative reduction of approximately 1–1.3% from the nominal resonance frequency (~20 kHz), indicating a temperature-induced decrease in effective dynamic stiffness. The trend is consistent across all cooling conditions, suggesting that resonance frequency is governed primarily by material and system stiffness rather than external cooling parameters. This behavior confirms the strong thermo-mechanical coupling in the system and highlights the necessity of continuous resonance tracking during testing. The relationship between excitation level and displacement amplitude, grouped by temperature ranges, is shown in **Figure 5**. At low temperatures (30–40 °C), displacement increases rapidly with excitation, indicating efficient energy transfer.

However, as temperature increases, the response becomes progressively nonlinear, with reduced displacement gains for equivalent increases in excitation. At higher temperatures (80–120 °C), a clear saturation behavior is observed, where displacement amplitude approaches a plateau despite increasing excitation levels. This behavior reflects diminishing returns in displacement due to reduced material stiffness and increased internal dissipation at elevated temperatures.

Displacement efficiency, defined as the ratio of displacement amplitude to excitation level (µm/VPP), is plotted as a function of temperature in **Figure 6**. A strong inverse relationship is observed.

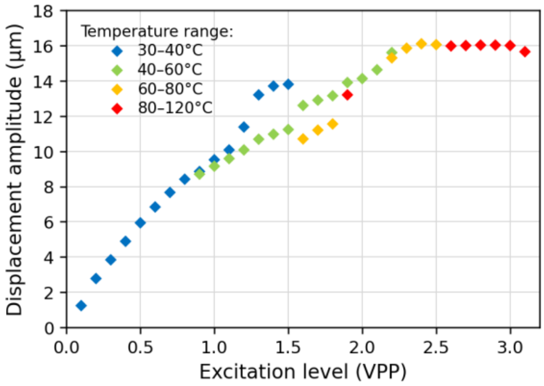

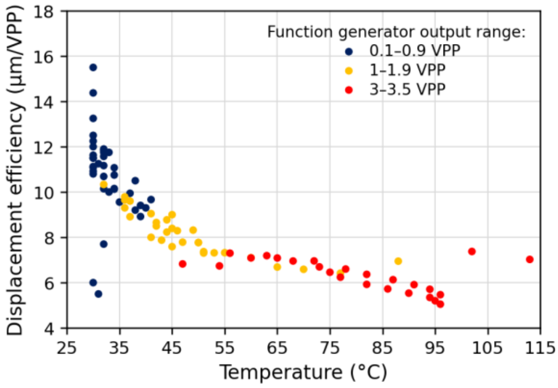

Figure 5 Displacement amplitude as a function of excitation level for different temperature ranges

Figure 6 Displacement efficiency as a function of specimen temperature for different excitation levels

At low temperatures (~30 °C), displacement efficiency reaches values above 12–14 µm/VPP, indicating highly efficient energy conversion. As temperature increases, efficiency decreases significantly, reaching values as low as approximately 5–7 µm/VPP at temperatures above 90 °C. The effect is more pronounced at higher excitation levels, where thermal softening and increased damping reduce the mechanical response. This confirms that displacement efficiency is not constant but strongly temperature-dependent, and therefore cannot be used as a fixed calibration parameter. The sensitivity of displacement amplitude to phase difference is shown in **Figure 7**, obtained during backward phase sweeps at constant excitation level.

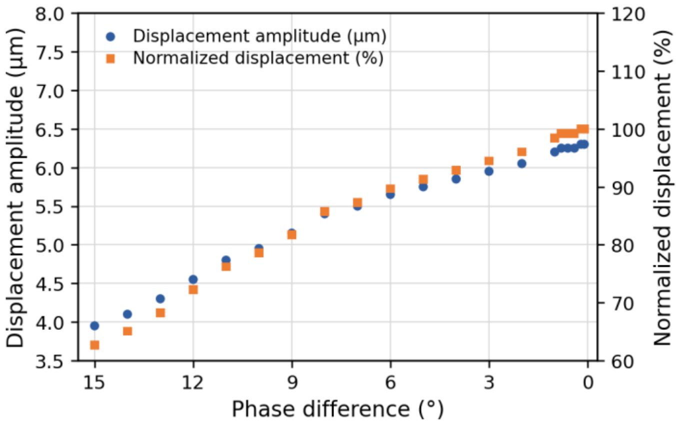

Figure 7 Displacement amplitude and normalized displacement as a function of phase difference

Displacement amplitude increases monotonically as phase difference decreases toward zero, reaching a maximum of approximately 6.3 µm at phase values near 0.1–0.2°. Rather than exhibiting a sharp peak, the system displays a plateau in displacement near resonance, indicating nonlinear resonance behavior. A stable high-amplitude region, defined as ≥95% of maximum displacement, is observed within a narrow phase window of approximately 0–2°. Outside this range, displacement decreases rapidly, demonstrating strong sensitivity of system response to phase variations. This confirms that resonance in the ultrasonic system is not defined by a single frequency but by a finite phase window, and that phase-controlled operation is essential for maintaining stable high-amplitude conditions.

4. CONCLUSION

Specimen temperature increased nonlinearly with excitation level, reaching above 100 °C and causing a resonance frequency reduction of approximately 200–250 Hz (1–1.3%), indicating decreased dynamic stiffness. Displacement amplitude exhibited nonlinear behavior with clear saturation at elevated temperatures, requiring higher excitation to maintain equivalent amplitudes. Displacement efficiency (µm/VPP) decreased significantly with temperature, demonstrating that it cannot be treated as a constant calibration parameter. A strong phase dependence was observed, with maximum displacement occurring near 0° and stable operation confined to a narrow phase window of approximately 0–2°. The presence of a plateau near resonance indicates nonlinear system behavior and highlights the importance of phase-controlled excitation. Overall, the results confirm that ultrasonic fatigue response is governed by coupled thermo-mechanical and phase-dependent effects, requiring temperature- and phase-aware calibration for reliable VHCF testing.

REFERENCES

[1] ZHAO, M., WU, T., ZHAO, Z., LIU, L., LUO, G., CHEN, W. Ultrasonic fatigue device and behavior of high-temperature superalloy Inconel 718 with self-heating phenomenon. *Applied Sciences*. 2020, 10, 8761. DOI: https://doi.org/10.3390/app10238761.

[2] MAYER, H. Recent developments in ultrasonic fatigue. *Fatigue & Fracture of Engineering Materials & Structures*. 2016, 39, 3–29. DOI: https://doi.org/10.1111/ffe.12365.

[3] SCHÖNBAUER, B.M., FITZKA, M., JASKARI, M., JÄRVENPÄÄ, A., MAYER, H. Very high cycle fatigue data acquisition using high-accuracy ultrasonic fatigue testing equipment. *Materials Performance and Characterization*. 2023, 12(2), 172–185. DOI: https://doi.org/10.1520/MPC20220113.

[4] SAFARI, S., MONTALVÃO, D., DA COSTA, P.R., REIS, L., FREITAS, M. Statistical calibration of ultrasonic fatigue testing machine and probabilistic fatigue life estimation. *International Journal of Fatigue*. 2025, 199, 109028. DOI: https://doi.org/10.1016/j.ijfatigue.2025.109028.

[5] ISTOMIN, K., DÖNGES, B., SCHELL, N., CHRIST, H.-J., PIETSCH, U. Analysis of VHCF damage in a duplex stainless steel using hard X-ray diffraction techniques. *International Journal of Fatigue*. 2014, 66, 177–182. DOI: https://doi.org/10.1016/j.ijfatigue.2014.04.001.

[6] FURUYA, Y., HIRUKAWA, H., TAKEUCHI, E. Gigacycle fatigue in high strength steels. *Science and Technology of Advanced Materials*. 2019, 20(1), 643–656. DOI: https://doi.org/10.1080/14686996.2019.1610904.